ELSEVIER

Use of Large-Footprint Scanning Airborne Lidar To Estimate Forest Stand Characteristics in the Western Cascades of Oregon

Joseph E. Means, Steven A. Acker,* David J. Harding,† J. Bryan Blair,† Michael A. Lefsky,‡ Warren B. Cohen,‡ Mark E. Harmon,* and W. Arthur McKee**

A scanning lidar, a relatively new type of sensor which explicitly measures canopy height, was used to measure structure of conifer forests in the Pacific Northwest. SLICER (Scanning Lidar Imager of Canopies by Echo Recovery), an airborne pulsed laser developed by NASA which scans a swath of five 10-m diameter footprints along the aircraft's flightpath, captures the power of the reflected laser pulse as a function of height from the top of the canopy to the ground. Ground measurements of forest stand structure were collected on 26 plots with coincident SLICER data. Height, basal area, total biomass, and leaf biomass as estimated from field data could be predicted from SLICER-derived metrics with r^2 values of 0.95, 0.96, 0.96, and 0.84, respectively. These relationships were strong up to a height of 52 m, basal area of 132 m^2/ha and total biomass of 1300 Mg/ha. In light of these strong relationships, large-footprint, airborne scanning lidar shows promise for characterizing stand structure for management and research purposes. ©*Elsevier Science Inc., 1999*

*Department of Forest Science, Oregon State University, Corvallis
†Laboratory for Terrestrial Physics, NASA Goddard Space Flight Center, Greenbelt, Maryland
‡USDA Forest Service, Forestry Sciences Laboratory, Pacific Northwest Research Station, Corvallis

Address correspondence to S. A. Acker, Oregon State University, Dept. of Forest Science. Forestry Sciences Lab. 020, Corvallis, OR 97331-7501. E-mail: ackers@fsl.orst.edu

Received 10 April 1998; revised 4 September 1998.

INTRODUCTION

Structural descriptions of forests are crucial to understanding how forest ecosystems function. In particular, information on broad-scale patterns of mass and vertical canopy structure would help advance studies of the global C cycle (Post, 1993), forest productivity (Ryan and Yoder, 1997), use of forest canopy habitats by birds (MacArthur, 1958), arboreal mammals (Carey, 1996), and arthropods (Schowalter, 1995), interactions between forests and streams (Gregory et al., 1991), and prediction of the behavior of wildfires in the canopy (Rothermel, 1991).

Although fine-scale studies have demonstrated the influence of structural characteristics on function, applying this knowledge at broad scales has been problematical because information on broad-scale patterns of vertical canopy structure has been very difficult to obtain. Passive remote sensing tools such as the Thematic Mapper cannot provide detailed height, total biomass, or leaf biomass estimates beyond early stages of succession in forests with high leaf area or biomass. Using Landsat TM data for example, Cohen et al. (1995) could only distinguish two structural classes for forests older than 80 years.

Past efforts to characterize the vertical dimension of forest canopies include diagrams of transects based on ground measurements (e.g., Ashton and Hall, 1992), probing with telephoto camera lenses to develop a canopy height profile (Aber, 1979; Brown and Parker, 1994; MacArthur and Horn, 1969; Parker et al., 1989), and measurement of vertical light profiles (Bolstad and Gower, 1990; Wang et al., 1992). These techniques can

REMOTE SENS. ENVIRON. 67:298–308 (1999)

655 Avenue of the Americas, New York, NY 10010

0034-4257/99/$–see front matter
PII S0034-4257(98)00091-1

be useful for small areas but are too time-consuming for use over large areas.

Current methods of characterizing vertical canopy structure over large areas include SAR (synthetic aperture radar) and lidar (light detection and ranging). SAR offers promise for predicting low levels of forest biomass and for mapping general forest types and tree species in floristicly simple landscapes (Rignot et al., 1994). However, SAR is insensitive to differences in forest biomass above 150 Mg/ha, well below values for many tropical and temperate forests (Waring et al., 1995).

A more promising method is airborne, scanning lidar which sends laser pulses toward the ground and measures the return time for reflections off vegetation surfaces and the ground (Flood and Gutelius, 1997; Lefsky, 1997; Weishampel et al., 1996). This allows estimation of vegetation height and other canopy-related characteristics. The first lidars used small footprints, usually 1 m diameter or smaller, and recorded reflections from a single track along the flightpath (Aldred and Bonnor, 1985; Nelson et al., 1984, 1988; Ritchie et al., 1993, 1992; Weltz et al., 1994). Small-footprint lidar can provide accurate canopy height estimates in some cases, for example in forests sufficiently sparse to allow identification of individual trees (e.g., Jensen et al., 1987). Recent studies, however, show that in denser forests small-footprint lidars tend to underestimate stand height (Nilsson, 1996; Naesset 1997a; though see "grid approach" in Naesset, 1997a). The underestimates of canopy height by small-footprint lidar may be due to failure to obtain reflections from the ground in areas of dense canopy closure and failure to sample the tops of relatively broad trees (Harding et al., 1994). Recent NASA instruments (Blair et al., 1994; Harding et al., 1994) capture reflections over a larger footprint, about 10 m in diameter, resulting in more complete sampling of the canopy, even for dense canopies (Weishampel et al., 1996). These profiling lidars have shown promise in estimating stand height, bole volume, woody biomass, and tree canopy cover.

This article presents results from a field test of an airborne lidar called SLICER (Scanning Lidar Imager of Canopies by Echo Recovery). SLICER uses a 10-m footprint and measures five adjacent, cross-track footprints along the flightpath, thus scanning a swath 50 m wide. SLICER evolved from a profiling system (Blair et al., 1994) by incorporation of a galvanometer mechanism for scanning the transmitted laser beam perpendicular to the direction of the flight path. Our goal is to evaluate the utility of data from SLICER for estimating canopy height, stand biomass, foliage biomass, and other stand structural characteristics. In particular, we wanted to test whether we could resolve differences in these characteristics at high levels of total aboveground and foliage biomass. Conifer forests of the Pacific Northwest, with leaf areas indices over 10 m^2/m^2 (Marshall and Waring, 1986) and live biomass over 1000 Mg/ha (Waring and Franklin, 1979) corresponding to volumes of up to 2500 m^3/ha, are an ideal place for such a test.

METHODS

Study Area

The study was conducted in and near the H.J. Andrews Experimental Forest, in the western Cascade Range, Oregon, USA. The study area is dominated by coniferous forest, primarily of Douglas-fir (*Pseudotsuga menziesii* (Mirbel) Franco) and western hemlock (*Tsuga heterophylla* (Raf.) Sarg.) (Dyrness et al., 1974). Old-growth forests in the study area can be quite massive (500–1000 Mg/ha aboveground live biomass, Grier and Logan, 1977) and tall (up to 80 m, Kuiper, 1988). Leaf area index (LAI) values up to 8 m^2/m^2 have been reported for old-growth forests in the study area (Marshall and Waring, 1986). In addition to old-growth forest (greater than 200 years old), the study area also includes abundant mature forest (80–200 years old), as well as areas regrowing following harvesting which began in the 1950s (Van Cleve and Martin, 1991). The Andrews Experimental Forest has been an intensive site for forestry, hydrology, and ecological research for nearly 50 years (Van Cleve and Martin, 1991).

The SLICER Instrument

SLICER is a scanning, airborne lidar that transmits short (ca. 120 cm, 4 ns) pulses of near infrared (1064 nm) laser light towards the ground using a laser transmitter specifically designed for surface lidar applications (Coyle and Blair, 1995; Coyle et al., 1995). Pulses are typically emitted at a repetition rate of 80 Hz and a power of 0.7 mJ. As a pulse encounters the top of the vegetation photons intercepted by canopy surfaces are scattered; photons backscattered at nadir are collected by a receiving telescope in the aircraft. As the non-intercepted component of the pulse proceeds down through the canopy, photons are backscattered at every level at which they encounter reflective surfaces. Finally, photons are usually reflected back to the collecting telescope from the ground in sufficient number to yield a detectable ground return signal. Received photons collected by the telescope are focused on a silicon avalanche photodiode detector which converts input optical energy into an output voltage signal. The round-trip travel time from transmission of the laser pulse to the first return of detector output voltage above a detection threshold is measured by a time interval unit (TIU). The travel time is converted to distance based on the speed of light. The TIU utilizes a high-frequency oscillator to achieve cm-level ranging accuracy. Upon reception of the first detected return signal, the time history of detector output voltage, which is sampled using an analog-to-digital digitizer (LeCroy 6880B operating at 1.35 Gsamp/s), is stored as a return waveform. The wave-

form contains 600 samples of the detector output signal at a sampling interval of 0.742 ns (i.e., 11 cm vertical sampling). The waveform records 15 channels of instrument noise occurring prior to reception of the first return above threshold, and 585 channels after the first return, yielding a digitized height range of 65 m downward from the canopy top.

SLICER was flown in a twin engine Sabreliner T-39 at about 5000 m above the ground for this study, yielding laser footprints nominally 10 m in diameter. Aircraft attitude is provided by a ring-laser gyro inertial navigation system. Aircraft position is determined by means of ground and aircraft-mounted dual frequency GPS receivers from which a postflight kinematic trajectory is derived. Knowing the position (*X*, *Y*, *Z*) and attitude of the aircraft and the round-trip time to each reflecting surface, the horizontal position of the first reflecting surface in each pulse is determined to within 5–10 m. Specific data collection lines were flown by means of a real-time GPS navigation system which displays the aircraft's position to the pilot relative to pre-programmed flight lines.

Two sampling transects were flown across and beyond the Andrews Experimental Forest in 1995. The maximum detectable tree height of 65 m prevented derivation of tree heights in a small percentage of laser footprints that included taller trees.

Field Sampling Design

To test the predictive power of SLICER over the full ranges of height, biomass, and foliage mass in the study area, ground plots were located in 1996 along the SLICER transects to include sites ranging from those devoid of all but herbaceous vegetation to old-growth forest. Multiple plots were located in bare or herb-covered areas (n=2), shrub-covered areas (n=3), young forest (20–80 years old, n=7), mature forest (n=5), and old-growth forest (n=9).

To help choose and find potential plot locations, Arc/View was used to combine: locations of the SLICER transects, a map of stand conditions (including establishment year), a forest type classification (Cohen et al., 1995), a false-color infrared Thematic Mapper image, and data layers of roads and streams. A total of 62 candidate plots were identified from which 26 plots were selected. Plots were selected for sampling after field verification that they met the following criteria: capable of supporting coniferous forest, only one predominant story or age class, basal area of broad-leaved trees $\leq$10%, slopes $<$90% for crew safety concerns, and shrub understory not heavy enough to obscure moosehorn densiometer measurements.

Field Methods

At each selected location a 50×50 m square plot was established. Each plot was oriented so as to correspond to 25 SLICER footprints and was centered on the center footprint. The main plot and 25 circular 10-m diameter subplots were slope corrected (i.e., plots were laid out using horizontal distances so that nominal plot areas are equal to plot areas projected to the horizontal plane). The subplots were distributed systematically throughout the main plot in a 5×5 grid.

The field crew first reconnoitered each candidate plot to verify that it fit the selection criteria. They then established an approximate plot center and obtained a GPS fix. After differential correction in the laboratory of the GPS fix for the approximate plot center, the plot center was repositioned as needed to place the center of the field plot at the coordinates of the target SLICER footprint. The accuracy of matching field plot centers with target SLICER footprints is estimated to be 5–20 m, a combination of an estimated 5–10 m error in SLICER footprint location, and 5–10 m error in corrected GPS location. Thus the field plots and sets of 25 SLICER footprints overlap and comprise samples of the same stands, though not necessarily the exact same pieces of ground. The uncertainty in the degree of overlap between the SLICER footprints and the field plots introduces presumably random errors into the estimated relationships between ground and SLICER data. The magnitude of errors should be greatest for the old-growth plots, inasmuch as old-growth forests tend to be more spatially heterogeneous than young and mature forests in the Pacific Northwest (Kuiper, 1988; Bradshaw and Spies, 1992).

The intensity of field sampling was a function of the type of stand sampled. On old-growth plots all trees greater than 1.37 m tall were measured. On other plots where density of trees was high, all trees greater than 1.37 m tall were measured on selected subplots. Initially, tree diameters were measured on three or five subplots. The field crew then estimated the number of additional subplots needed to include at least 30 dominant and codominant trees [i.e., trees forming the main canopy (Avery and Burkhart, 1994)], and measured trees on five, nine, or 13 subplots, regularly spaced to cover the full extent of the plot.

For all measured trees, species, DBH (diameter at 1.37 m above the ground), and crown ratio (estimated proportion of tree height with live branches around at least 1/3 of the circumference of the bole) were recorded. To develop species-specific regression models of height and sapwood thickness on DBH, intensive measurements were taken on a subsample of trees. For each tree species with more than 10 individuals on a given plot, 10 individuals were chosen spanning the range of DBH on the plot. From each of these trees two cores were taken for bark thickness and sapwood thickness, and total height was measured with a Suunto clinometer and distance measuring device. Use of height-DBH regressions is a practical alternative to exhaustive height

measurements for the dense coniferous forests of the Pacific Northwest (Garman et al., 1995); sampling constrained to include the entire range of DBH, rather than to include a random sample of trees, ensures that the resulting regression models can be applied to all trees in a study without extrapolation (e.g., Curtis and Marshall, 1986).

Tree canopy cover was estimated with the moosehorn densiometer (Bunnell and Vales, 1990) at the center of each of the 25 subplots. The moosehorn was used because its narrow view angle approximates SLICER's near-vertical sampling.

Shrubs, herbs, and trees less than 1.37 m tall were measured only if canopy cover by moosehorn was less than 40%, which occurred on five plots. We reasoned that understory total and leaf biomass would not be important to the total in stands with significant tree cover. This vegetation was measured as follows. On the five corner and center subplots cover of all vascular plant species was estimated, including trees <1.37 m tall. Cover of species >1.37 m tall was recorded along 10-m-long line intercept transects through the subplot centers. In addition, basal stem diameters of erect shrubs were measured in a 50-cm-wide strip on the uphill side of the line intercept.

SLICER Data Analysis Methods

Initial processing at NASA's Goddard Space Flight Center provided latitude, longitude, and elevation of the first return (tree canopy top) and the return waveform. The waveforms were further processed with software adapted from a program written for SLICER data from eastern deciduous forests (Lefsky, 1997). Several quantities defined below were computed for each footprint.

The lidar-derived metrics were ground elevation, canopy height, canopy height profile, median canopy height, canopy reflection sum, ground reflection sum, and canopy closure. Ground elevation is the elevation of the peak or mode of the last return in the waveform, inferred to be a reflection from the ground. The ground returns on several footprints on old-growth plots had to be adjusted with reference to adjacent waveforms due to complete ground shading by heavy overstory or loss of part or all of the ground return because of the termination of waveform recording at 65 m from the first return. Canopy height is the distance from the first return to the ground. Canopy height profile (CHP) was calculated by correcting the returned energy profile for shading of lower foliage by higher foliage using a modified exponential transformation (MacArthur and Horn, 1969; Lefsky, 1997), which assumes uniform horizontal distribution of foliage. Canopy reflection sum is the sum of the portion of the waveform return reflected from the canopy. Ground reflection sum is the sum of the portion of the waveform return reflected from the ground multiplied by a factor of 2 to approximately correct for an assumed lower reflectivity at 1064 nm of the litter-covered ground as compared to the canopy. Canopy closure is canopy reflection sum divided by the sum of canopy and ground reflection sums.

The assumption of uniform horizontal distribution of foliage is not met in our conifer forests, because lower foliage is often under higher foliage in the same crown and gaps of various sizes extend to the ground or nearly so. Thus CHP's probably do not represent the true vertical distribution of foliage in these stands. However, we believe metrics derived from the CHP are potentially useful in predicting stand characteristics.

The lidar-derived metrics were averaged over all footprints in a plot for comparison to field data. The CHP's for all footprints in a plot were aligned by their ground returns and averaged. Median canopy height was calculated from the mean CHP as the height at which half of the area under the CHP was above and half was below. Quadratic mean canopy height (QMCH) was defined as mean canopy height weighted by the square of the distance from the ground, and was calculated from the mean CHP.

Calculation of Field-Based Stand Characteristics

From the field data, plot-level biomass was estimated using allometric equations on DBH and sapwood cross-sectional area for trees, and cover and basal diameter for herbs and shrubs. For trees, allometric equations on DBH from Means et al. (1994) were used to compute most components of aboveground biomass. Foliage biomass of trees was estimated from allometric equations on sapwood cross-sectional area. The three predominant tree species were Douglas-fir, western hemlock, and western redcedar (*Thuja plicata* Donn). For Douglas-fir and western hemlock, sapwood cross-sectional area of cored trees was first regressed on DBH separately for the two species (Douglas-fir: $r^2=0.80$, $n=221$; western hemlock: $r^2=0.85$, $n=111$). The resulting models were used to estimate sapwood cross-sectional area for all trees. Tree foliage biomass was then calculated using published sapwood area to leaf area ratios (Waring et al., 1982) and specific leaf areas (Gholz et al., 1976; Waring et al., 1982). For small trees (i.e., Douglas-firs <13 cm DBH and western hemlock <14 cm DBH), foliage mass was estimated from allometric equations on DBH (Gholz et al., 1979; Helgerson et al., 1988), since there was an inadequate sample of small trees that had been cored.

Estimation of foliage mass of western redcedar was based on a published data set of sapwood thickness and DBH (Lassen and Okkonen, 1969), a published allometric equation for foliage mass as a function of DBH (Gholz et al., 1979), and western redcedars on our plots for which sapwood thickness and DBH were measured. For the range of DBH used in constructing the allomet-

Table 1. Characteristics of the Field Plots Based on Field Data, Summarized by Seral Stage[a]

Seral Stage[b]	*N*[c]	*Trees per ha*	*Mean DBH (cm)*	*Mean Height (m)*[d]	*Tree Basal Area (m^2/ha)*	*Tree Foliage Biomass (Mg/ha)*	*Total Above-Ground Biomass (Mg/ha)*
B	2	0	n/a	n/a	0	0	2 (2)
S	3	1282 (1024)	3 (2)	4 (2)	2 (2)	1 (1)	15 (10)
Y	7	1975 (942)	12 (5)	17 (2)	32 (9)	9 (2)	213 (67)
M	5	948 (737)	32 (19)	33 (6)	57 (13)	10 (1)	493 (172)
O	9	689 (286)	29 (13)	43 (6)	92 (20)	12 (3)	965 (174)

[a] Values are means, with standard deviations in parentheses.
[b] B=bare, S=shrub, Y=young forest, M=mature forest, O=old-growth forest.
[c] Number of plots representing the seral stage.
[d] Mean of predicted heights of codominant and dominant trees.

ric equation, foliage mass was computed from the allometric equation and sapwood area was calculated from the published data set. A mean ratio of foliage mass to sapwood area was then computed, weighted by the number of trees in different size classes in the published data set. Finally, using the trees with sapwood measurements, predicted foliage mass (i.e., observed sapwood area times mean foliage mass:sapwood area ratio) was regressed on DBH (r^2=0.85, n=51). From this model, foliage mass was estimated from DBH for all western red cedars ≥16 cm DBH. For smaller trees foliage mass was estimated directly from the allometric equation, since the sample of small trees that had been cored was insufficient, and the regression model underpredicted foliage mass for very small trees.

Mean canopy height was calculated using species-specific height–DBH relationships derived from measured heights. For western hemlock and western redcedar separate regressions of height on DBH were developed using data from all plots for dominant and codominant trees (western hemlock: r^2=0.75, n=57; western red cedar: r^2=0.60, n=19). For Douglas-fir three separate regressions were developed for trees in young, mature, and old-growth plots (young: r^2=0.74, n=73; mature: r^2= 0.78, n=34; old-growth: r^2=0.57, n=77). For each plot the heights of dominant and codominant trees were predicted using the regression models, and then averaged. Plot canopy cover was the mean of the 25 moosehorn readings.

Statistical Methods

Relationships between plot-level SLICER metrics and stand characteristics were investigated with interactive graphical and regression techniques (SAS, 1996). Transformations of independent variables included square root, square, standard deviation, and coefficient of variation among footprints on a plot. Logarithmic transformations of dependent variables were also explored.

RESULTS

Twenty-six plots were located in and near the Andrews Experimental Forest. The sampled stands covered a wide range of height and biomass values (Table 1). The highest stand biomass (1329 Mg/ha), foliage biomass (17.2 Mg/ha), and basal area (132 m^2/ha) are among the highest found in a region known for its high biomass values (Means and Helm, 1985).

Douglas-fir was the most dominant and ubiquitous tree species, averaging 76% of basal area (range 38–100%) on plots with trees. Western hemlock was the second most ubiquitous species, occurring on 21 of 24 plots with trees and accounting for an average of 18% of tree basal area on those plots. Western red cedar, golden chinkapin (*Castanopis chryosphylla* (Dougl.) DC), western dogwood (*Cornus nuttalli* Aud.), and western yew (*Taxus brevifolia* Nutt.) occurred on about half of the plots with trees. Nine other tree species occurred less frequently.

It was possible to predict a wide variety of stand structural characteristics from SLICER data (Table 2). Mean SLICER-derived height was a good predictor of mean canopy height through the full range of heights observed (Fig. 1, Eq. (1) in Table 2). The slope was significantly less than 1.0, indicating the SLICER-derived height is consistently greater than the field-based height. The intercept is close to zero and not significant (p=0.85), indicating that the model is realistic for short stands. No other candidate predictor was significant when added to the regression model.

Basal areas were quite high in old-growth and mature stands (Table 1). There was a strong relationship between basal area and SLICER-derived height (Table 2, Eq. (2)), although there is more scatter for greater heights. The best two-predictor model includes canopy reflection sum as a predictor (Table 2, Eq. (3)). At advanced ages, height growth rate decreases greatly (King, 1966; Means and Helm, 1985), and thus height loses some of its power as a predictor of basal area. Canopy reflection sum presumably serves as a measure of the quantity of foliage (although woody canopy elements also reflect the laser light), and so helps identify the stands with higher basal area.

Total stand biomass was closely related to the square of SLICER-derived canopy height (Fig. 2, Eq. (5) in Ta-

Table 2. Relationships between Ground-Based Stand Structural Characteristics (Dependent Variables) and SLICER–Derived Metrics from Regression Analysis[a]

Eq. No.	*Ground data*[b]	*Predictive model based on SLICER measurements*[c]	r^2	*RMSE*
1	Ht (m)	0.3+0.91∘LHt (Fig. 1)	0.95	3.8
2	BA (m^2/ha)	5.3+1.97∘LHt	0.88	13
3	BA	$1.1+0.0279\circ LHt^2+13.9\circ CanRef^2$	0.92	11
4	BA	$1.1+0.0411\circ LHt^2+13.5\circ CanRef^2-0.0389\circ QMCH^2$	0.96	9
5	TotBio (Mg/ha)	$55.+0.385\circ LHt^2$ (Fig. 2)	0.90	132
6	TotBio	$48.+0.576\circ LHt^2-0.573\circ QMCH^2$	0.94	103
7	TotBio	$-23.+0.539\circ LHt^2-0.553\circ QMCH^2+69.4\circ CanRef^2$	0.96	88
8	FolBio (Mg/ha)	−0.64+0.0026∘CanRef (Fig. 3)	0.84	2.0
9	FolBio[d]	12.7−0.0021∘GndRef	0.67	1.3
10	FolBio[e]	−14.2+0.00095∘CanRef	0.81	1.5
11	CanCov	0.14+0.995∘CanClos	0.94	0.08
12	CanCov[f]	$0.58+0.38\circ CanClos^2$	0.53	0.06
13	CanCov[f]	$-0.68+0.47\circ CanClos^2-0.040\circ MedCanHt^{0.5}$	0.69	0.05

[a] Sample size=26 except as noted.
[b] Ht=mean canopy height, BA=basal area, TotBio=total above ground stand biomass, FolBio=foliage biomass, CanCov=canopy cover (range 0–1).
[c] LHt=mean canopy height derived from lidar data, CanRef=canopy reflection sum, QMCH=quadratic mean canopy height, CanClos=canopy closure, GndRef=ground reflection sum, MedCanHt=median canopy height.
[d] Plots with trees, with LHt≤35 m. $N=10$.
[e] Plots with trees, with LHt>35 m. $N=11$.
[f] Plots with trees. $N=21$.

ble 2). The best two- and three-predictor models (Eqs. (6) and (7), respectively, in Table 2), gave significantly better fits. These relationships extended to stands with very high biomass (1100–1300 Mg/ha), although there is more variability not accounted for by the models for such high levels of biomass.

Tree foliage biomass was best predicted by canopy reflection sum (Eq. (8) in Table 2, Fig. 3). Since most of this relationship was caused by the difference between the plots with no trees (bare and shrub) and those with trees (young, mature and old-growth), models for tree foliage biomass in the subset of plots with trees ($n=21$) were investigated. Different models worked better for plots with mean SLICER-derived height ≤35 m and for plots with mean SLICER-derived height >35 m (Table 2, Eqs. (9) and (10)). Using two separate models for all plots with trees gave a significantly better fit ($\alpha=0.05$) than using one model.

Ground-based canopy cover of trees was closely related to SLICER-derived canopy closure (Table 2, Eq. (11)). The Y-axis intercept was not significantly different from 0.0, and the slope was not significantly different from 1.0. Since most of the strength of this relationship was caused by the difference between the plots without tree cover (bare and shrub) and those with (young, mature, and old-growth), models for tree canopy cover in the subset of plots with trees were investigated. The best single-predictor relationship found was a function of SLICER canopy closure (Table 2, Eq. (12)), and a two-predictor model improved the r^2 to 0.69. Efforts to build different models for subsets of the plots did not improve the fit.

Figure 1. Mean height of dominant and codominant trees estimated from field data versus SLICER-derived height. The regression line is Eq. (1) in Table 2.

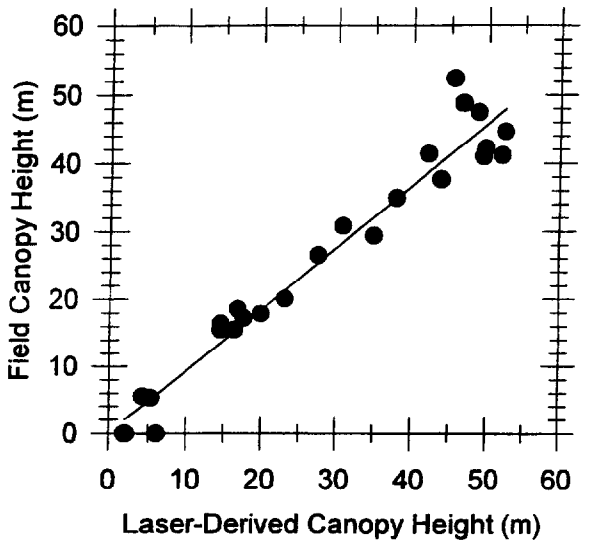

DISCUSSION

Prediction of Stand Structure

Data from SLICER can be used to accurately predict important stand structural characteristics in the tall coniferous forests of the Pacific Northwest. This ability extends to very high values of stand and foliage biomass.

The relationship between mean SLICER height and mean height of dominant and codominant trees estimated from field data was strong (Fig. 1). However, the slope was significantly less than 1.0, indicating that SLICER-derived heights were greater than field-derived heights. Part of this discrepancy is likely to be due to a

methodological difference between canopy height measurement with SLICER versus field observation. Canopy height from SLICER was determined for each plot by averaging the maximum canopy height in each of 25 footprints. From field data, stand height was computed as the average height of all trees that were judged to compose the main canopy layer (i.e., dominant and codominant trees). Given the density of dominant and codominant trees, this estimate from the field data included many trees which would have been too short to produce the first return in a SLICER footprint. For example, in the 13 plots in which all trees were measured, the median sample size of tree heights used to estimate canopy height was 41. Since there is considerable within-stand variability in heights of dominant and codominant trees in coniferous forests in the Pacific Northwest (see, e.g., Kuiper, 1988), the relatively large sample sizes used to estimate canopy height from the field data depressed those estimates relative to the estimates derived from SLICER. An artifact of height measurement with SLICER may have made a smaller contribution to the discrepancy between the two canopy height estimates. The tree producing the first return in a given footprint is most likely to be on the upslope side of the footprint, so that its height would be overestimated in the SLICER data by the difference in elevation between its base and the peak of the ground return.

The strong relationship between SLICER height and stand basal area is not surprising because forest yield tables, for example, for Douglas-fir (McArdle et al., 1961) consistently show strong relationships between height and basal area. Inclusion of SLICER height and canopy reflection sum in the two-parameter model allows a better fit for plots with high basal areas. In this model canopy reflection sum can be interpreted as an index of stocking, or the extent to which the canopy growing space is occupied by trees.

The strong relationship between stand height and stand biomass (Fig. 2) also occurs in yield tables (McArdle et al., 1961). The mature stands have relatively low volumes for their heights compared to the old-growth stands and thus contribute to error in the one-parameter model. These stands also have foliage mostly in the upper half of the canopy, and so have relatively high QMCH values. The inclusion of QMCH with a negative coefficient in the two-parameter model allows this source of variation to be explained.

The ability of canopy reflection sum to predict foliage biomass (Fig. 3) is also as expected. It is surprising, however, that canopy reflection sum gives a better fit than SLICER-derived canopy closure because total energy varies from pulse to pulse, and this variation is removed from canopy closure by dividing by total returned energy. The relatively poor explanatory power of SLICER-derived canopy closure may be caused by variability in ground reflectivity. Variability in proportions of the ground covered by vegetation versus litter could alter total returned energy inasmuch as vegetation has about twice the reflectivity of litter.

Interestingly, the relationship between SLICER-derived and field measures of the same canopy feature, that is, canopy closure, was not as strong as that between biomass and SLICER-derived canopy metrics. Conceptually, the moosehorn densiometer views the canopy

Figure 2. Total aboveground biomass as estimated from field data versus the square of SLICER-derived height. The regression line is Eq. (5) in Table 2.

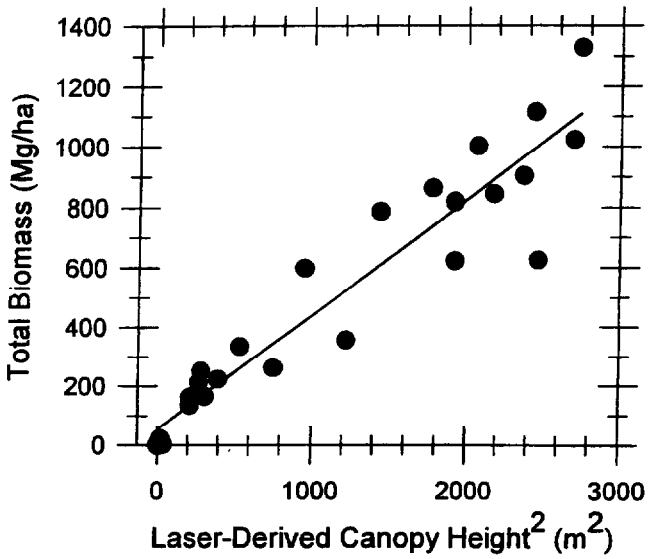

Figure 3. Tree foliage biomass as estimated from field data versus canopy reflection sum. The regression line is Eq. (8) in Table 2.

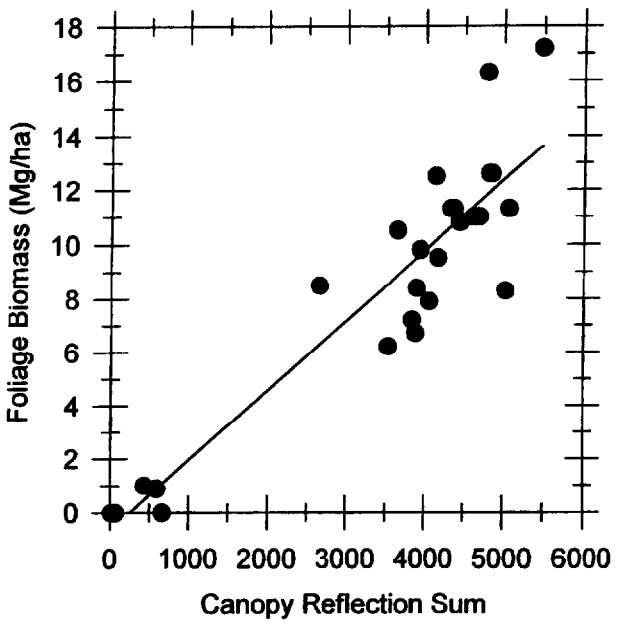

from below at the same angle as SLICER does from above. However, as computed in this study, canopy closure is a function of canopy reflection sum, that is, energy reflected from all layers in the canopy. In contrast, moosehorn measurements take into account only layers of foliage closest to the observer.

Potential Uses of Large-Footprint Scanning Airborne Lidar

Large-footprint scanning airborne lidar has important potential uses in forested landscapes. This study indicates that large-footprint scanning airborne lidar can accurately map biomass and carbon stores and so can be used to validate landscape simulation models (Cohen et al., 1992). This study also shows that large-footprint lidar can estimate accurately height and foliage biomass, so that it can help map these features for initialization of such landscape simulation models. Current approaches to estimating carbon balances of the heavily forested Pacific Northwest rely on coarse vegetation classes to estimate current height and biomass (Cohen et al., 1996) that could be improved significantly with lidar data.

SLICER's ability to characterize canopy structure in three dimensions makes scanning airborne lidar a logical choice to map arboreal habitat. Views of three-dimensional features and patterns of canopies have been impossible to obtain over large areas. Primarily for this reason, although much is known about response of important arboreal animals such as the spotted owl and marbled murrelet to two-dimensional habitat patterns, little is known about their response to three-dimensional patterns. Lidar has the potential to help fill this gap.

Data from scanning airborne lidars can be used to characterize tree height, tree diameter, and the shade environment of riparian zones, since tree height can be related to tree diameter (Garman et al., 1995) They can characterize canopy fuels and provide detailed (10 m) topography needed to simulate crown fires, which are the most difficult wildfires to understand (Rothermel, 1991).

Airborne lidar data are complementary to passive remote sensing data, such as Landsat Thematic Mapper. TM can be used to distinguish bare, shrub, and early tree stages of succession well (Cohen et al., 1995; Cohen and Spies, 1992), but large-footprint airborne lidars are unlikely to be able to separate these on steep slopes due to spreading of the ground return. Lidar is uniquely capable of characterizing taller vegetation with higher total and foliage biomass where relationships between passively-sensed spectral data and biomass and foliage saturate and passive remote sensing provides relatively little discriminating ability.

In future applications of large-footprint lidar over larger areas the manual adjustments of the ground returns for several waveforms in this study are not likely to be necessary. The instrument settings that limited the maximum detectable tree height in this study to 65 m can be altered so that the maximum detectable tree height exceeds 100 m (Blair et al., 1994).

Comparison to Small-Footprint Lidar

Although large- and small-footprint lidar overlap somewhat in their capabilities for measuring forest structure, there are significant differences between the two types of lidar in technical features, data obtained, and availability of data.

Both small- and large-footprint lidars show promise for estimating stand height and volume or biomass. Although small-footprint lidars tend to underestimate canopy height, this problem may be alleviated, at least for relatively short-statured forests, by selecting the largest height estimate from all laser pulses corresponding to a fixed ground area (Naesset, 1997a), or by employing sophisticated algorithms for analysis of waveforms for those instruments capable of capturing complete waveforms (Nilsson, 1996). The magnitude of bias in lidar height estimates in this study (mean=+2.3 m) is similar to those reported for small-footprint lidars (i.e., −5.5 m to +1.9 m in Nilsson, 1996, and Naesset, 1997a). The variability of differences between tree heights estimated with lidar and measured from the ground was greater in this study (s.d.=4.0 m) than reported by Naesset (1997a) for small-footprint lidar (s.d.=1.1–1.6 m). However, this study included a range of heights that is about three times as great as the range in the study reported by Naesset. Furthermore, comparisons between SLICER and the small-footprint lidars concern not only different types of lidar technology but also different methods of summarizing ground data. As described above, the overestimate of height in this study might be alleviated by averaging ground-measured heights over a smaller number of trees more likely to correspond to the tallest individuals responsible for the first returns in SLICER waveforms. The coefficients of determination for total stand biomass in this study (i.e., 0.9–0.96) are greater than recently reported coefficients of determination for volume prediction from small-footprint lidar (i.e., 0.47–0.89 in Nilsson, 1996 and Naesset, 1997b).

Important technical differences distinguish large-footprint and small-footprint lidars in their currently most common implementations. Small-footprint airborne lidars typically operate in the near infrared at 300–7000 laser pulses per second (Flood and Gutelius, 1997) and scan swath widths of up to 730 m corresponding to off-nadir scan angles up to 20° (Wagner, 1995). With differentially corrected GPS and either a stabilized aircraft platform or an aircraft with an inertial navigation system, small-footprint lidars generate data point locations with an accuracy of 15 cm in three dimensions under optimal conditions (Wagner, 1995; Flood and Gutelius, 1997). Small-footprint lidars can be programmed to collect the

first return (reflection) or the last return (Wagner, 1995), but most do not provide continuous return waveforms. A small-footprint lidar with the potential to record entire waveforms has been tested for measuring tree heights and stand volume (Nilsson, 1996). However, data storage limitations prevented recording of complete waveforms for most of its measurements. Though published studies are not available on performance of small-footprint lidars in tall, dense, coniferous forests with high leaf areas, we anticipate that their canopy penetration may be limited at higher scan angles. This could limit effective swath width for some purposes. However, given the positive results for estimating stand height and volume cited above, study of small-footprint lidar in tall-coniferous forest is warranted.

The key distinction between SLICER and small-footprint lidars is SLICER's broad footprint. Due to the broad footprint, reflections from the top of the canopy are recorded for all pulses except those that fall in larger gaps, and reflections from the ground through small holes in the canopy are recorded for all but the most dense canopies. Thus almost all pulses provide a canopy height measurement and information on the vertical structure of the canopy (Harding, et al., 1994). Other important features of SLICER include the relatively short and sharp pulse of laser energy, the receiver's ability to accommodate a large dynamic range of return signals, and digitization of the return signal (Blair et al., 1994). The resulting full waveform of the reflected pulse provides a top-to-bottom view of dense canopies and makes possible additional analyses of canopy structure (Lefsky, 1997).

The two types of lidar contrast in their availability. Small-footprint lidars are becoming widely available commercially (Flood and Gutelius, 1997). The most common uses of commercial small-footprint airborne lidar are topographic mapping and surveying of structures such as buildings and power lines (Flood and Gutelius, 1997). However, at least one widely available commercial lidar has been tested for measurements of forest structure (Naesset, 1997a,b).

SLICER and other large-footprint lidars from NASA (see Blair and Coyle, 1996; Garvin et al., 1998) are research instruments and have collected data for limited areas only. At present we know of no commercial operators of large-footprint scanning lidar. However, data from large-footprint lidar will soon become much more widely available. In the year 2000, NASA in collaboration with the University of Maryland, will launch the Vegetation Canopy Lidar (VCL) (Dubayah et al., 1997). Over its 2-year lifetime, this satellite-borne instrument is planned to acquire data over 3–5% of the Earth's land area between 65° N and S latitude. The orbit of the satellite has been designed so that VCL will sample nearly all the major forest and woodland types on Earth. Data from this instrument will be available to the public (Dubayah et al., 1997).

We are grateful to Bob Burns, Barry Coyle, Earl Frederick, David Pierce, George Postel, David Rabine, and Virgil Rabine for their invaluable efforts in acquiring the SLICER data, and to Kathy Still for producing the geolocated SLICER products. Development of SLICER was funded by NASA's Solid Earth Program and Goddard's Directors Discretionary Fund. Acquisition of the SLICER data used in this study was supported by NASA's Terrestrial Ecology Program. To Scott Miller, Crystal Dickard, Becky Fasth, Matthew Goslin, and Kerry Halligan, we are grateful for collecting field data under difficult conditions. We thank also two anonymous reviewers for many constructive comments on the manuscript. This work was supported by the National Science Foundation (Award No. DEB-9011663, Amendment No. 11).

REFERENCES

Aber, J. D. (1979), A method for estimating foliage-height profiles in broad-leaved forests. *J. Ecol.* 67:35–40.

Aldred, A. H., and Bonnor, G. M. (1985), Application of airborne laser to forest surveys, Information Report PI-X-51, Can. For. Serv., Petawawa National Forestry Inst., Chalk River, 62 pp.

Ashton, P. S., and Hall, P. (1992), Comparisons of structure among mixed dipterocarp forests of northwestern Borneo. *J. Ecol.* 80:459–481.

Avery, T. E., and Burkhart, H. E. (1994), *Forest Measurements.*, 4th ed. McGraw-Hill, New York, 408 pp.

Blair, J. B., and Coyle, D. B. (1996), Vegetation and topography mapping with an airborne laser altimeter using a high-efficiency laser and a scannable field-of view telescope. In *Proceedings of the Second International Airborne Remote Sensing Conference and Exhibition*, Environ. Research Inst. Michigan, Vol. II, pp. 403–407.

Blair, J. B., Coyle, D. B., Bufton, J. L., and Harding, D. J. (1994), Optimization of an airborne laser altimeter for remote sensing of vegetation and tree canopies. In *Proceedings of IGARSS'94 Conference*, Pasadena, CA, 8–12 August, pp. 939–941.

Bolstad, P. V., and Gower, S. T. (1990), Estimation of leaf area in fourteen southern Wisconsin forest stands using a portable radiometer. *Tree Physiol.* 7:115–124.

Bradshaw, G. A., and Spies, T. A. (1992), Characterizing canopy gap structure in forests using wavelet analysis. *J. Ecol.* 80:205–215.

Brown, M. J., and Parker, G. G. (1994), Canopy light transmittance in a chronosequence of mixed-species deciduous forests. *Can. J. For. Res.* 24:1694–1703.

Bunnell, F. L., and Vales, D. J. (1990), Comparison of methods for estimating forest overstory cover: differences among techniques. *Can. J. For. Res.* 20:101–107.

Carey, A. B. (1996), Interactions of Northwest forest canopies and arboreal mammals. *Northwest Sci.* 70(Special Issue): 72–78.

Cohen, W. B., and Spies, T. A. (1992), Estimating structural attributes of Douglas-fir/western hemlock forest stands from Landsat and SPOT imagery. *Remote Sens. Environ.* 41:1–17.

Cohen, W. B., Wallin, D. O., Harmon, M. E., Sollins, P., Daly, C., and Ferrell, W. K. (1992), Modeling the effect of land use on carbon storage in the forests of the Pacific North-

west. In *Proceedings of IGARSS'92 Conference*, Houston, TX, 26–29 May, pp. 1023–1026.

Cohen, W. B., Spies, T. A., and Fiorella, M. (1995), Estimating the age and structure of forests in a multi-ownership landscape of western Oregon, U.S.A. *Int. J. Remote Sens.* 16: 721–746.

Cohen, W. B., Harmon, M. E., Wallin, D. O., and Fiorella, M. (1996), Two decades of carbon flux from forests of the Pacific Northwest. *BioScience* 46:836–844.

Coyle, D. B., and Blair, J. B. (1995), Development of a Q-switched/cavity dumped, sharp pulsed laser transmitter (SPLT) for airborne altimetry. In *Optical Society of America Proceedings on Advanced Solid-State Lasers*, Vol. 24, pp. 5–8.

Coyle, D. B., Guerra, D. V., and Kay, R. B. (1995), An interactive numerical model of diode-pumped, Q-switched/cavity dumped lasers. *J. Phys. D: Appl. Phys.* 28:452–462.

Curtis, R. O., and Marshall, D. D. (1986), Levels-of-growing-stock cooperative study in Douglas-fir, Report No. 8, The LOGS study: twenty-year results, Research Article PNW-356, Pacific Northwest Research Station, USDA Forest Service, Portland, OR, 113 pp.

Dubayah, R., Blair, J. B., Bufton, J. L., et al. (1997), The Vegetation Canopy Lidar mission. In *Proceedings, Land Satellite Information in the Next Decade II: Sources and Applications*, Am. Soc. for Photogramm. and Remote Sens., Bethesda, MD, pp. 100–112.

Dyrness, C. T., Franklin, J. F., and Moir, W. H. (1974), A preliminary classification of forest communities in the central portion of the western Cascades in Oregon, Coniferous Forest Biome Bull. No. 4, Univ. of Washington, Seattle, 123 pp.

Flood, M., and Gutelius, B. (1997), Commercial implications of topographic terrain mapping using scanning airborne laser radar. *Photogramm. Eng. Remote Sens.* 63:327–366.

Garman, S. L., Acker, S. A., Ohmann, J. L., and Spies, T. A. (1995), Asymptotic height-diameter equations for twenty-four tree species in Western Oregon, Research Contribution 10, Forest Research Laboratory, Oregon State University, Corvallis, 22 pp.

Garvin, J., Bufton, J., Blair, J., et al. (1998), Observations of the Earth's topography from the Shuttle Laser Altimeter (SLA): laser-pulse echo-recovery measurements of terrestrial surfaces. In *Physics and Chemistry of the Earth*, in press.

Gholz. H. L., Fitz, F. K., and Waring, R. H. (1976), Leaf area differences associated with old-growth forest communities in the western Oregon Cascades. *Can. J. For. Res.* 6:49–57.

Gholz. H. L., Grier, C. C., Campbell, A. G., and Brown, A. T. (1979), Equations for estimating biomass and leaf area of plants in the Pacific Northwest, Research Article 41, Forest Research Laboratory, Oregon State University, Corvallis, 37 pp.

Gregory, S. V., Swanson, F. J., McKee, W. A., and Cummins, K. W. (1991), An ecosystem perspective of riparian zones. *BioScience* 41:540–551.

Grier, C. C., and Logan, R. S. (1977), Old-growth *Pseudotsuga menziesii* communities of a western Oregon watershed: biomass distribution and production budgets. *Ecol. Monog.* 47:373–400.

Harding, D. J., Blair, J. B., Garvin, J. B., and Lawrence, W. T. (1994), Laser altimetry waveform measurement of vegetation canopy structure. In *Proceedings of IGARSS'94 Conference*, Pasadena, CA, 8–12 August, pp. 1251–1253.

Helgerson, O. T., Cromack, K., Stafford, S., Miller, R. E., and Slagle, R. (1988), Equations for estimating aboveground components of young Douglas-fir and red alder in a coastal Oregon plantation. *Can. J. For. Res.* 18:1082–1085.

Jensen, J. R., Hodgson, M. E., Jackey, H. E., Jr. and Krabill, W. (1987), Correlation between aircraft MSS and LIDAR remotely sensed data on a forested wetland. *Geocarto Int.* 4:39–54.

King, J. E. (1966), Site curves for Douglas-fir in the Pacific Northwest, Weyerhaeuser Forestry Article 8, Forest Research Center, Weyerhaeuser Co., Centralia, WA, 49 pp.

Kuiper, L. C. (1988), The structure of natural Douglas-fir forests in western Washington and western Oregon, Agricultural University Wageningen Articles, 88-5, pp. 1–47.

Lassen, L. E., and Okkonen, E. A. (1969), Sapwood thickness of Douglas-fir and five other western softwoods, Research Article FPL-124, U.S. Forest Service, Forest Products Laboratory, Madison, WI, 16 pp.

Lefsky, M. A. (1997), Application of lidar remote sensing to the estimation of forest canopy and stand structure, Ph.D. thesis, University of Virginia, 185 pp.

MacArthur, R. H. (1958), Population ecology of some warblers of northeastern coniferous forests. *Ecology* 39:599–619.

MacArthur, R. H., and Horn, H. S. (1969), Foliage profile by vertical measurements. *Ecology* 50:802–804.

Marshall, J. D., and Waring, R. H. (1986), Comparison of methods of estimating leaf-area index in old-growth Douglas-fir. *Ecology* 67:975–979.

McArdle, R. E., Meyer, W. H., and Bruce, D. (1961), The yield of Douglas-fir in the Pacific Northwest, Technical Bulletin 201, U. S. Department of Agriculture, Washington, DC, 74 pp.

Means, J. E., and Helm, M. E. (1985), Height growth and site index curves for Douglas-fir on dry sites in the Willamette National Forest, Research Article PNW-341, Pacific Northwest Research Station, USDA Forest Service, Portland, OR, 17 pp.

Means, J. E., Hansen, H. A., Koerper, G. J., Alaback, P. B., and Klopsch, M. W. (1994), Software for computing plant biomass—BIOPAK users guide, General Technical Report PNW-GTR-340, Pacific Northwest Research Station, USDA Forest Service, Portland, OR, 184 pp.

Naesset, E. (1997a), Determination of mean tree height of forest stands using airborne laser scanner data. *ISPRS J. Photogramm. Remote Sens.* 52:49–56.

Naesset, E. (1997b), Estimating timber volume of forest stands using airborne laser scanner data. *Remote Sen. Environ.* 61:246–253.

Nelson, R., Krabill, W., and Maclean, G. (1984), Determining forest canopy characteristics using airborne laser data. *Remote Sens. Environ.* 15:201–212.

Nelson, R., Krabill, W., and Tonelli, J. (1988), Estimating forest biomass and volume using airborne laser data. *Remote Sens. Environ.* 24:247–267.

Nilsson, M. (1996), Estimation of tree heights and stand volume using an airborne lidar system. *Remote Sens. Environ.* 56:1–7.

Parker, G. G., O'Neill, J. P., and Higman, D. (1989), Vertical

profile and canopy organization in a mixed deciduous forest. *Vegetatio* 85:1–11.

Post, W. M. (1993), Uncertainties in the terrestrial carbon cycle. In *Vegetation Dynamics and Global Change* (A. M. Solomon and H. H. Shugart, Eds.), Chapman and Hall, New York, pp. 116–132.

Rignot, E., Way, J., Williams, C., and Viereck, L. (1994), Radar estimates of aboveground biomass in boreal forests of interior Alaska. *IEEE Trans. Geosci. Remote Sens.* 32: 1117–1124.

Ritchie, J. C., Everitt, J. H., Escobar, D. E., Jackson, T. J., and Davis, M. R. (1992), Airborne laser mesurements of rangeland canopy cover and distribution. *J. Range Manage.* 45: 189–193.

Ritchie, J. C., Evans, D. L., Jacobs, D., Everitt, J. H., and Weltz, M. A. (1993), Measuring canopy structure with an airborne laser altimeter. *Trans. Am. Soc. Agric. Eng.* 36: 1235–1238.

Rothermel, R. C. (1991), Predicting behavior and size of crown fires in the northern Rocky Mountains, Research Article INT-438, USDA Forest Service, Intermountain Research Station, Fort Collins, CO, 46 pp.

Ryan, M. G., and Yoder, B. J. (1997), Hydraulic limits to tree height and tree growth. *BioScience* 47:235–242.

SAS (1996), SAS System for Windows, Release 6.12, SAS Institute Inc., Cary, NC.

Schowalter, T. D. (1995), Canopy arthropod communities in relation to forest age and alternative harvest practices in western Oregon. *For. Ecol. Manag.* 78:115–125.

Van Cleve, K., and Martin, S., Eds. (1991), *Long-Term Ecological Research in the United States*, 6th ed., rev., LTER Network Office, University of Washington, Seattle, 178 pp.

Wagner, M. J. (1995), Seeing in 3-D without the glasses. *Earth Obs. Mag.* 4(7):51–53.

Wang, Y. S., Miller, D. R., Welles, J. M., and Heisler, G. M. (1992), Spatial variability of canopy foliage in an oak forest estimated with fisheye sensors. *For. Sci.* 38:854–865.

Waring, R. H., and Franklin, J. F. (1979), Evergreen coniferous forests of the Pacific Northwest. *Science* 204:1380–1386.

Waring, R. H., Schroeder, P. E., and Oren, P. (1982), Application of the pipe model theory to predict canopy leaf area. *Can. J. For. Res.* 12:556–560.

Waring, R. H., Way, J., Hunt, E. R., Jr., et al. (1995), Imaging radar for ecosystem studies. *BioScience* 45:715–723.

Weishampel, J. F., Ranson, K. J., and Harding, D. J. (1996), Remote sensing of forest canopies. *Selbyana* 17:6–14.

Weltz, M. A., Ritchie, J. C., and Fox, H. D. (1994), Comparison of laser and field measurements of vegetation height and canopy cover. *Water Resour. Res.* 30:1311–1319.